Delaminated areas beneath organic coating: A local electrochemical impedance approach

Jean-Baptiste Jorcin, Emmanuel Aragon, Céline Merlatti and Nadine Pébère

Centre Inter Universitaire de Recherche et d'Ingénierie des Matériaux, UMR CNRS 5085, ENSIACET, 118, Route de Narbonne, 31077 Toulouse Cedex 04, France
UPRES 1356 "Matériaux à Finalités Spécifiques", Université du Sud Toulon Var, ISITV, BP 56, Avenue Georges Pompidou, 83162 La Valette du Var Cedex, France

Abstract

Local electrochemical impedance mapping was used to investigate delamination phenomena at the steel/epoxy-vinyl primer interface. The delamination occurred from an artificial defect (cutter scribing) and from ageing in a salt spray chamber. The samples were taken from the salt spray chamber after 20, 30 and 50 days of exposure. To observe delamination after ageing, the corrosion product layers were removed by a cathodic polarization at −1.5 V/SCE for 4 h. A non-aged reference sample was tested for comparison. Mapping was performed at 5 kHz. Initiation and propagation of the delamination were clearly observed. The delaminated surface areas measured by visual observations after the removal of the coating were lower than those determined by local electrochemical impedance mapping. The delamination mechanisms were discussed with reference to literature data.

Keywords: Steel; LEIS; Coatings; Delamination

1. Introduction

Organic coatings are widely used to prevent corrosion of metallic structures because they can easily be applied at a reasonable cost. It is generally accepted that the coating efficiency is dependent on the intrinsic properties of the organic film (barrier properties), on the substrate/coating interface in terms of adherence, on the inhibitive or sacrificial pigments included in the primer and on the degree of environment aggressiveness.

In marine corrosion, one of the main objectives is to increase the durability of organic coatings to fifteen years and more. Thus, the long-range forecast of organic coatings and the characterisation of the ageing state in service constitute key technological goals. Moreover, for environmental and human health considerations, the development of low toxicity paints (water-based paints) has become a priority. As yet, no correlation has been established between the resistance in service and results obtained in laboratories, which could allow, coating durability to be reliably predicted. As a matter of fact, for these new systems, there is a lack of feedback on their behaviour in actual use. Faced with this challenge, the strategy developed in different industries is the same:

(i) to perform correlation studies between accelerated ageing and natural ageing of a whole range of paint systems;

(ii) to develop fundamental research on the structures of polymers and on the mechanisms of ageing of the organic films by using techniques such as electrochemical impedance spectroscopy (EIS), scanning vibrating electrode technique (SVET), scanning Kelvin probe (SKP), Fourier transform infrared (FTIR) spectroscopy, differential scanning calorimetry (DSC) or dynamic mechanical analysis (DMA) to measure the glass transition temperature, adherence testing, etc.

Starting from these considerations, a study was performed on a large scale to develop an accelerated procedure of ageing to obtain a good estimation of the paint durability in a natural environment. In parallel, our intention was to obtain better knowledge of the degradation mechanisms as a function of exposure time. The present work constitutes part of this extensive project to study the correlation between natural or artificial ageing of paints. The aim of the study is to characterise the processes involved in the degradation of an organic coating from artificial defects and to assess the extent of delamination underneath the coating by a non-conventional method: local electrochemical impedance spectroscopy (LEIS). During the last decade, it has been demonstrated that LEIS is a powerful tool to investigate localised corrosion on bare metal surfaces and on coated alloys [1], [2], [3], [4], [5], [6], [7], [8], [9] and [10]. In a first step, the samples were characterised by conventional EIS.

2. Experimental

2.1. Samples

substrate consisted of carbon steel sheets (150 × 150 × 2 mm). The coating was an epoxy-vinyl primer with calcium ferrite, iron oxide and talc as pigments. It was applied on degreased and sand-blasted steel as defined in ISO 8501-1. Liquid paint was applied by air spraying and, after drying, the coating was about 80 μm thick. The corrosive medium was a NaCl solution in contact with air, quiescent and at ambient temperature. The concentration for the conventional impedance measurements was 0.1 M and the concentration was 0.001 M for the local impedance measurements. The local impedance measurements were carried out in a low conductivity medium (9.4×10^{-5} S cm^{-1}) to optimise resolution.

2.2. Ageing procedure

Two types of artificial defects were used for the study (Fig. 1). The first one was done manually with a cutting knife. The defect had a V-shaped profile. The second one was performed with a scribing machine using a drill bit of 2 mm diameter. Only the results obtained with cutter scribing were reported here. A preliminary study [11] reported the results obtained for the two types of scribing.

Fig. 1. Schematic representation of the two artificial defects: (a) cutter scribing and (b) machine scribing.

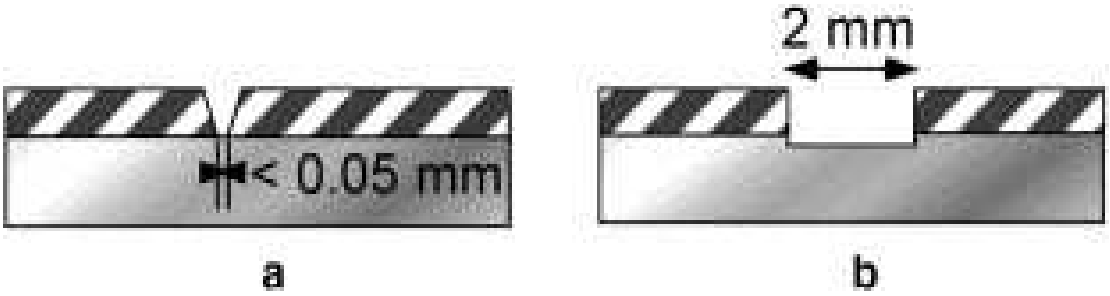

Ageing was performed in a salt spray chamber from which the samples were removed after 20, 30 and 50 days of exposure. A non-aged reference sample was tested for comparison.

2.3. Surface appearance

Visual sample observations showed, independently of the time of exposure to the salt spray, the existence of two different layers: an outer layer, brown, rusty and poorly adherent which is generally described as a mixture of iron hydroxides [12] and an inner layer, black and strongly adherent identified as a conducting layer of magnetite [12]. The thickness of the layers increased with the exposure time. You et al. [13] studying the corrosion of pure iron in an aerated 0.5 M NaCl solution showed, by in situ photographs, the presence of the same corrosion product layers which were also modified when the immersion time increased. Bousselmi et al. [14] and [15] have studied by electrochemical impedance spectroscopy the time-dependent modifications of the surface layers formed on a carbon steel exposed to natural water with high salt contents. Several layers were identified: the two layers previously described and an additional green rust layer (Fe(II)–Fe(III) hydroxysulfates) at the metal interface which was formed due to a high content of sulphate ions in the aggressive medium. Frateur et al. [16] have studied the cast iron/drinking water system by impedance and photographic observations. Qualitatively, the same corrosion products were observed.

After exposure to the salt spray chamber, the global and the local impedance responses were representative of the presence of corrosion products which covered the scratch and a large zone around the defect. Thus, the corrosion products masked the delamination. For conventional impedance, the samples were tested with the corrosion product layers. For

localised impedance, the corrosion products were removed by cathodic polarisation at −1.5 V/SCE for 4 h to observe delamination. It was assumed that the duration of the cathodic polarisation was short enough to avoid further coating delamination, which was then only due to the exposure to the salt spray.

2.4. Electrochemical measurements

For the classical EIS measurements, a three-electrode cell was used: the working electrode with an exposed area of 24 cm^2, a saturated calomel reference electrode (SCE) and a platinum auxiliary electrode. Electrochemical impedance measurements were performed using a Solartron 1287 electrochemical interface and a Solartron 1250 frequency response analyser in a frequency range of 65 kHz to a few mHz with eight points per decade using 10 mV peak-to-peak sinusoidal potential.

Localised electrochemical impedance spectroscopy (LEIS) was carried out with a Solartron 1275. This method used a five-electrode configuration (Fig. 2). LEIS measurements were made from the ratio of the applied AC voltage to the local AC current density. The applied voltage ($\Delta V_{applied}$) was the potential difference between the working electrode and the reference electrode. The local AC current density (i_{local}) was calculated using Ohm's law

$$i_{local} = \frac{\Delta V_{local}}{d} \times \kappa \quad (1)$$

where κ is the conductivity of the electrolyte and d the distance between the two probes positioned on and in a conical plastic holder: one protrudes from the tip of the cone and the other is a ring placed around the cone 3 mm from the tip.

Fig. 2. Schematic epresentation of the LEIS apparatus.

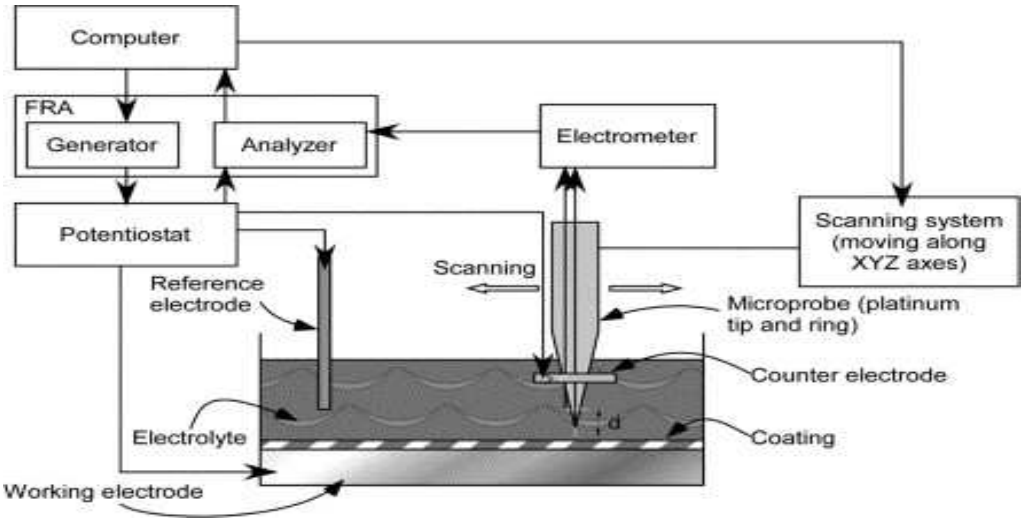

The local impedance Z_{local} is calculated by the relationship

$$Z_{local} = \frac{\Delta V_{applied}}{i_{local}} \quad (2)$$

For local electrochemical impedance mapping (LEIM): the probe was stepped across a designated area of the sample. In the present case, the analysed part was an area of 32 000 × 24 000 μm, above the active zone. The step size was 500 μm in the *X* and *Y* directions. Admittance was plotted rather than impedance to improve the spatial resolution of the mapping [11]. Two excitation frequencies were chosen: 5 kHz and 10 Hz. The value of 5 kHz was chosen to take into account the organic coating. The value of 10 Hz was chosen as a trade-off between quick scanning and the fact that the contribution of localised corrosion to the overall impedance is generally found in the low-frequency range. Here, only the plots at 5 kHz were reported because delamination was more visible at this frequency.

With the experimental set-up used, only the normal component of the current was measured and the area analysed was not accurately known. However, it was estimated to be about 1 mm^2 [17].

3. Results and discussion

Global and local impedance results are presented here for the coating in NaCl electrolyte.

3.1. Conventional impedance

Fig. 3 shows the conventional impedance diagram obtained for the coating in the absence of defects. This diagram is typical of a coated system. It can be recalled that the impedance spectrum was divided into two different parts: the high frequency part (HF) represents the properties of the coating and the low-frequency part (LF) the reaction occurring at the bottom of the pores of the coating [18]. In the very LF range (<150 mHz), the points are more scattered (not reported in the figure) due to the high impedance of the system. It can be assumed that the second time constant is also representative of the diffusion process of oxygen through the coating. From the first loop, the film capacitance was estimated to be about 0.2 nF cm^{-2}. This value agrees well with the order of magnitude for the capacitance of a film whose thickness is about 80 μm. A high impedance value measured in the LF range (1.2×10^8 Ω cm^2) indicates satisfactory protection.

Fig. 3. Conventional impedance diagram obtained for the coating without defect after 24 h of immersion in 0.1 M NaCl solution.

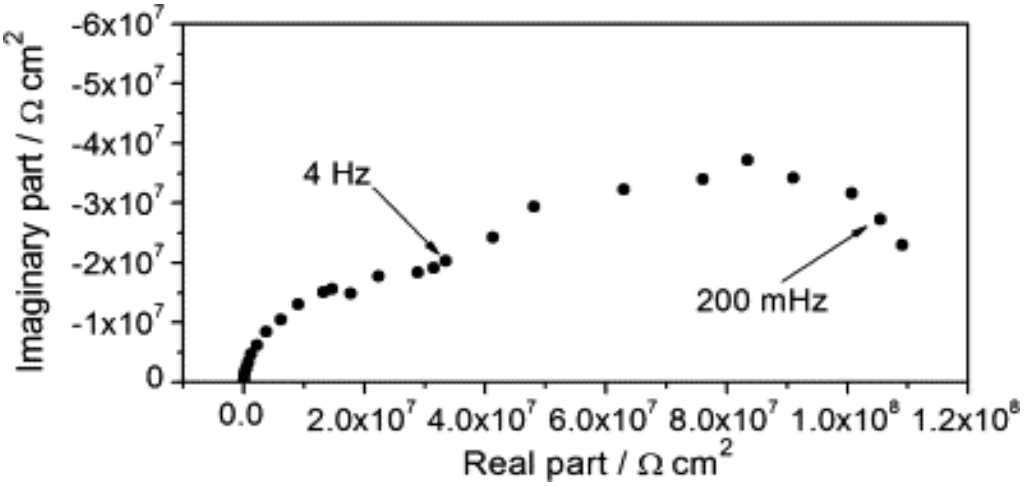

Then, global impedance spectra were recorded for the coated systems with the artificial defect and for different ageing times in the salt spray chamber (0, 20, 30 and 50 days). The results are reported in Fig. 4. The area of unprotected steel was sufficiently to

render the diagrams essentially representative of the processes occurring in the defect. As a consequence, the units in the figure are in Ω because the real surface area investigated is not accurately known. For the reference (without exposure in the salt spray chamber), a single capacitive loop is observed. The diagram characterises the corrosion of bare metal.

Fig. 4. Conventional impedance diagrams obtained for the epoxy-vinyl primer with an artificial defect (cutter scribe mark) after different durations of exposure in the salt spray chamber: (•) 0 day, (■) 20 days, (▲) 30 days, (⋆) 50 days.

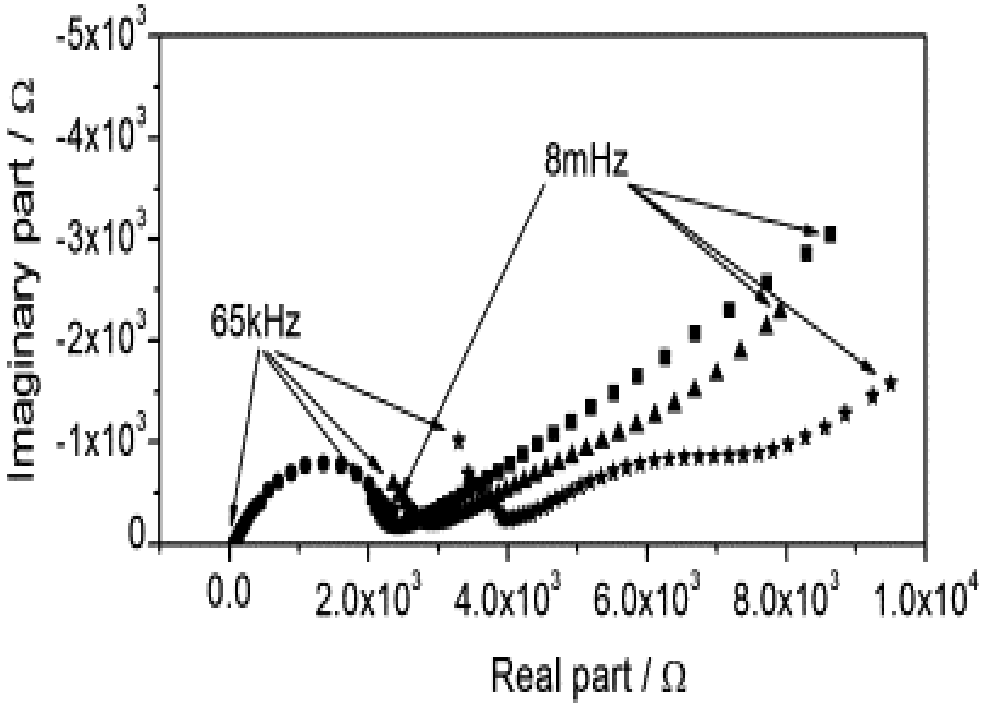

When the time of exposure to the salt spray increased, the corrosion spread out and the corrosion products sealed the scribe mark. The diagrams were strongly modified. They can be described by two or three loops depending on the exposure time. The first one, in the high frequency range, has a semi-circle shape, although all the points cannot be obtained due to the frequency domain used for the measurements. Given the low apparent value of the associated capacitance, the HF loop might reflect the response of a dielectric layer. The black layer of corrosion products (magnetite) cannot be distinguished from the metal by electrical measurements due to its good electric conductivity [14], [15] and [16] and thus, the HF impedance response must be that of the brown, rusty layer where diffusion controls the corrosion rate. All the global impedance diagrams were obtained in a 0.1 M NaCl solution, the HF resistance corresponds to the electrolyte resistance, R_e, which is the same,

independently of the ageing time. The HF part of the impedance diagrams after 20, 30 and 50 days of exposure to the salt spray chamber was fitted by a simple equivalent circuit composed of: the electrolyte resistance, R_e, which is fixed and measured with respect to the reference sample, in series with the film resistance, R_f, in parallel with the film capacitance, C_f. The capacitances were replaced by constant phase elements (CPE) to take into account the non-ideal behaviour of the interface [19].

The CPE_f is given by

$$Z_{CPE} = \frac{1}{Q(j\omega)^{\alpha}} \quad Q \text{ is in } \Omega^{-1}\ m^{-2}\ s^{\alpha}$$

α(CPE exponent) is related to the angle of rotation of a purely capacitive line on the complex plane plots. α is generally close to 1.

The film capacitance can be calculated by using the following equation [20]:

$$C_f = Q(R_e^{-1} + R_f^{-1})^{(\alpha-1)/\alpha} \quad C \text{ is expressed in Farads}$$

The values of the parameters are reported in Table 1. It can be seen that R_f increased and C_f decreased when the exposure time increased. This can be explained by the thickening of the corrosion product layer. However, it can be noted that α differs depending on the exposure time. This is correlated with the significant variation of the capacitance which decreased by a factor of 140 when the exposure time increased from 20 to 50 days. After 50 days of exposure the decrease of the capacitance can be explained by the modification of the dielectric properties of the corrosion products.

Table 1.

Parameters of the HF part of the impedance diagrams presented in Fig. 4

Exposure time (days)	R_e **(Ω)**	R_f **(Ω)**	α	C **(μF)**
0	80	–	–	–
20	80	2186	0.66	0.21
30	80	2400	0.79	0.012
50	80	3356	0.89	0.0015

In the low-frequency range, a linear part is observed which can be attributed to oxygen diffusion through the corrosion product layers. The high frequency part of the diffusion impedance has an angle of about 20–25° with respect to the real axis (25° for 30 days and 20° for 30 and 50 days). The same types of diagram were presented by Mattos and co-workers [21] for blistered samples after 10 years natural ageing and by van der Weijde et al. [22] on a coated panel with a blocked defect (100 μm). The flat appearance of the diagram could be attributed to the corrosion products which generated a more confined environment. In the case of a cast iron electrode, Frateur et al. [16] have modelled the flattened impedance spectra by the use of de Levie's porous electrode theory. After 50 days of exposure, a third time constant appeared in the medium frequency range. In relation with the significant decrease of the film capacitance, this behaviour would be linked to the modification of the properties of the corrosion products in the scratch after long exposure to the salt spray.

Looking at Fig. 4, it can be seen, from the global diagrams, that it is not possible to analyse the delamination process to determine the delaminated area. This result corroborates the conclusions presented by van der Weijde et al. [22] for EIS measurements on an artificial blister in organic coatings. They have shown that the corrosion products in the defect dominate the impedance characteristics, thus masking other contributions. In addition, they mentioned that the impedance of the corrosion product is high. This was also confirmed by our local impedance mapping. To observe delamination, it will be necessary to remove the corrosion products by a cathodic polarization. An attempt was made to measure the global impedance after the removal of the corrosion product layers to characterise the delamination. It was not possible to obtain the diagram in the absence of corrosion products because, for short immersion times, the system was not stationary and when the stationary state was reached, corrosion products had already formed in the scratch. Thus, local impedance spectroscopy was used.

3.2. Localised electrochemical impedance mapping (LEIM)

Fig. 5 presents LEI maps obtained for the coating with the artificial defect (cutter scribe mark) after different durations of ageing in the salt spray chamber. For 20 days of exposure, a step is clearly observed on the edge of the scribe, which increased with the ageing time. For 50 days of exposure, the step is no longer observed but baseline admittance is higher. This indicates that the studied zone is not large enough to visualise the step. Thus, delamination is significant. The delaminated surface areas measured by LEIM, and by visual

observation were compared. For the visual observations, the coating was removed after the electrochemical tests. Fig. 6 presents, as an example, a photograph of the sample after 30 days of exposure and after the removal of the coating. The delaminated zones measured by visual observation and by LEIM are shown by dotted lines in the figure. It can be seen that corrosion products are present around the scratch. Numerous blisters are also visualised near the corrosion products. The delaminated area measured by visual observation corresponds to the zone covered by the corrosion products and the blisters. It can be noticed that some blisters were observed far from the scratch (Fig. 5b) but no corrosion products were observed beneath these blisters.

Fig. 5. LEIM carried out at 5 kHz: (a) before exposure in the salt spray chamber and after different durations of exposure to the salt spray: (b) 20 days, (c) 30 days and (d) 50 days. Cutter scribe mark.

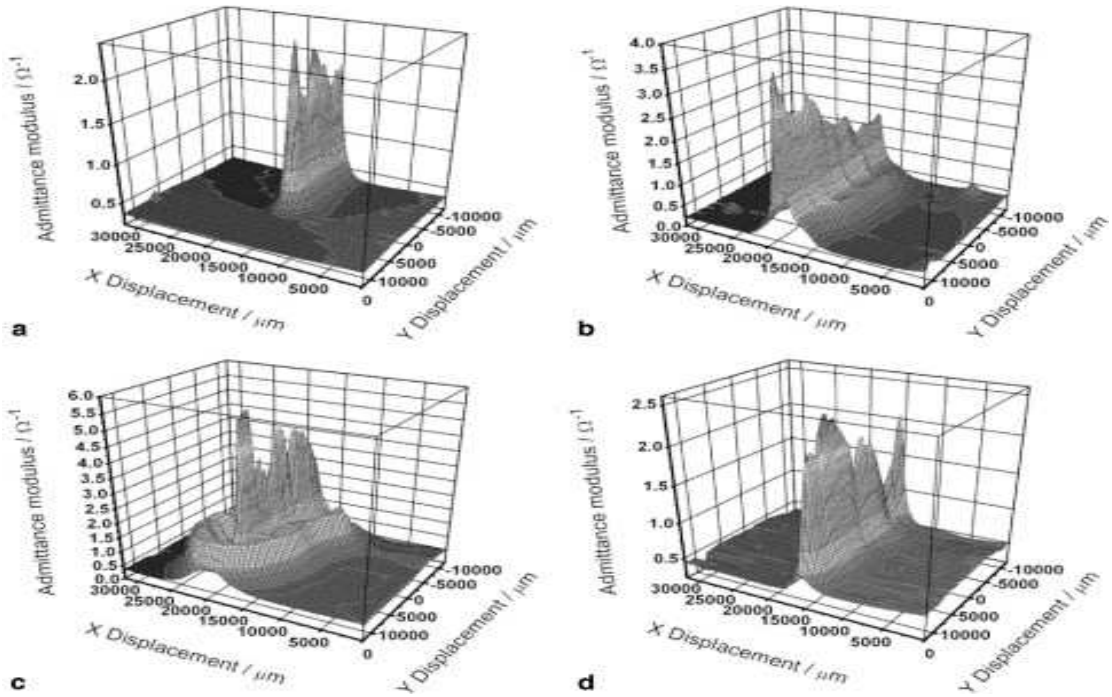

Fig. 6. Photograph of the scratched area after removal of the coating (30 days of exposure). The dotted lines correspond to the delaminated surface areas estimated from visual observation and from LEIM.

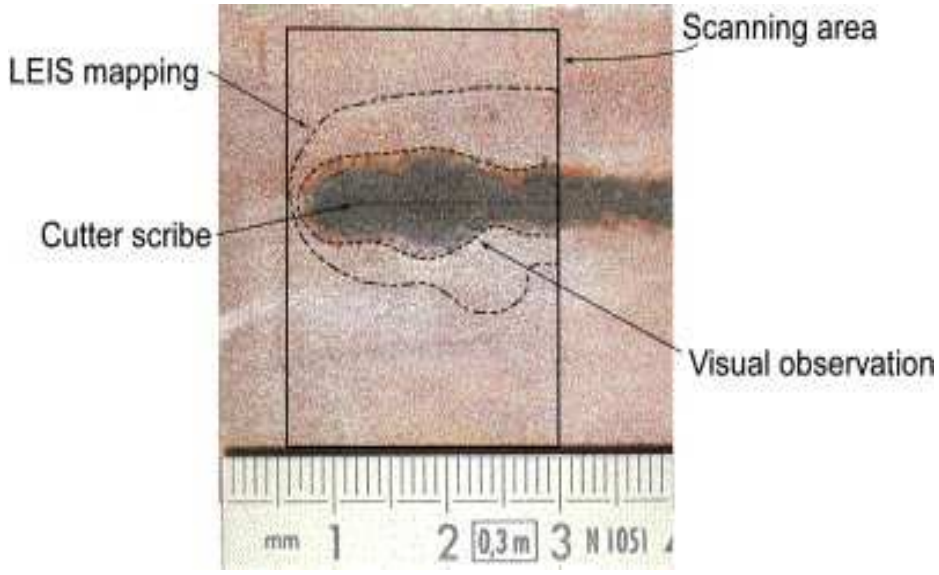

The presence of corrosion products corresponds, on the LEIM, to low admittance values (high impedance values). Around the corrosion products, and particularly after 30 and 50 days of exposure in the salt spray chamber, the LEIM presented high admittance values (low impedance). It can be assumed that the low impedance values correspond to loss of adherence of the organic coating. Thus, the delaminated area measured by LEIM corresponds to the limit of the high admittance values. It can be seen that the delaminated surface area measured by LEIM is significantly higher than that observed by visual examination.

Fig. 7 reports the variation of the delaminated surface area measured by visual observations and by LEIM after different durations of exposure in the salt spray chamber. The delaminated area increases as the exposure time increases. Although the surface areas are higher when they are measured by LEIM (between 2.1 and 2.5 times higher), the variation is quite similar. It must be emphasised that the error on the surface areas measured by LEIM is low because the spatial resolution of the probe, estimated around 1 mm^2, is low by comparison to the measured delaminated areas (>100 mm^2). Thus, the measurements were obtained with good accuracy. In Fig. 5, LEIM clearly reveals weak zones with poor adherence to the metal substrate around the corrosion products. It can be concluded that LEIM allowed the delamination process to be observed and quantified.

Fig. 7. Delaminated surface area as a function of exposure time to the salt spray estimated from: (•) visual observations after removal of the coating, (■) LEIM.

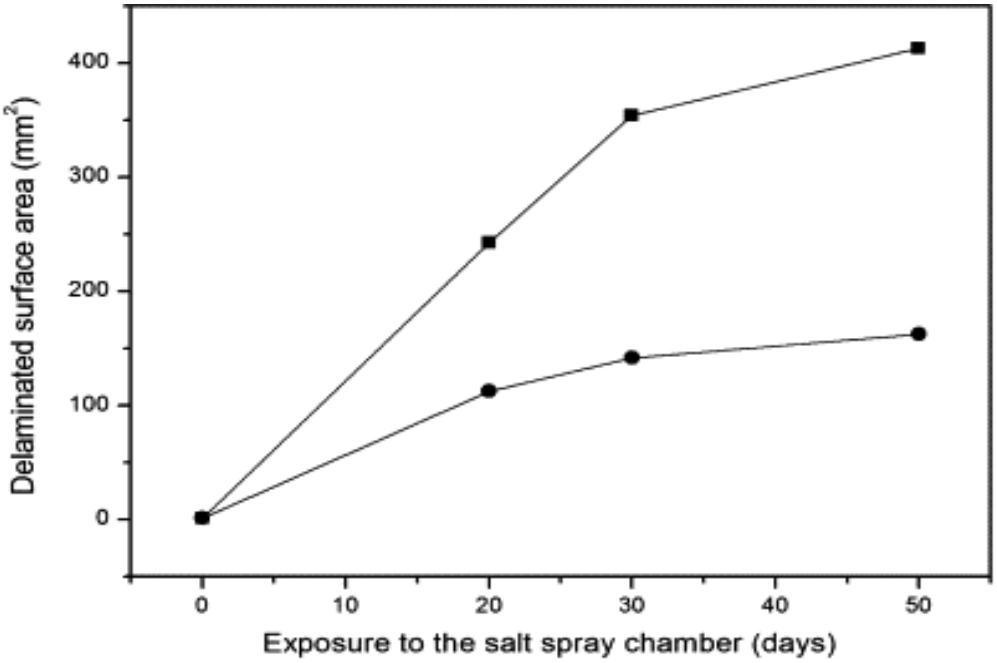

For the systems studied, the delamination mechanism can be described by reference to the works of Funke [23]. He described blistering of paint films and filiform corrosion and concluded that (i) the corrosion products and the process of their transformation with time influence the electrochemical corrosion process in and around the defect and (ii) the role of oxygen is determinant in the mechanism of delamination. Oxygen is consumed by the oxidation of the primary corrosion products and it is no longer available for the local corrosion cells to operate at the steel surface beneath. Therefore, these areas are polarized anodically and in turn give rise to the formation of cathodic areas in the neighborhood. This explains the formation of blisters at various locations in the coated system. The presence of blisters is also explained by the low film thickness, which allows water penetration, by an osmotic process. More recent papers describing cathodic delamination or anodic undermining confirmed these mechanisms [24].

A schema of the delamination mechanism is presented in Fig. 8 which accounts well for the results presented in Fig. 5:

(i) The corrosion products are formed at the scratch and spread out around it. According to Barton et al. [25], in the presence of chloride, fairly soluble ferrous chloride hydrate or hydroxy chlorides are formed (rusty layer). The transformation of these corrosion products to yield insoluble oxides, e.g. Fe_2O_3, by hydrolysis and oxidation (black layer) leads to the

release of chloride anions which can again participate in producing soluble primary corrosion products, thus enhancing the action of the local corrosion elements autocatalytically.

(ii) The region located under the corrosion products becomes anodic whereas the region under the coating becomes cathodic. Oxygen, which diffuses through the coating, can then be reduced to OH^-. Locally, the pH is significantly increased and delamination propagates.

(iii) The anodic zones advance due to the formation of corrosion products, increasing the area of oxygen reduction and thus propagating delamination under the coating.

Fig. 8. Schematic view of a section through a film showing the delamination process in the presence of a scribe mark.

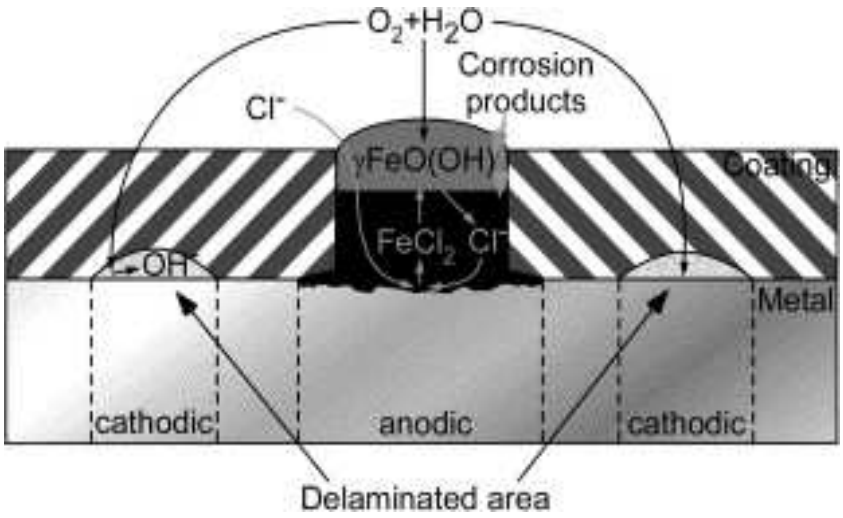

According to Funke [23], the basic principle of blister development is always the different availability of oxygen at various locations in the coated system, and is subject to change during exposure due to the formation of corrosion products.

4. Conclusions

LEIS was used to investigate delamination at the steel/organic coating interface. Initiation and propagation of delamination were clearly observed on industrial samples. This point is important because localised measurements are usually performed on small samples specially prepared for the particular technique used. For example, Scanning Kelving probe force microscopy developed by Rohwerder et al. [26] to study delamination, needs ultrathin polymer film and specially prepared defects. LEIM revealed the presence of the corrosion products beside the scratches (low admittance) and delaminated areas around (high admittance). The propagation of delamination noted here is in agreement with different studies reported in the literature. The development of the corrosion products in the scratch and diffusion of oxygen through the coating play important roles.

In the future, it will be necessary to obtain more information from local impedance spectra and also to establish the correlation between the results obtained with conventional impedance and localised impedance.

Acknowledgement

The authors thank Dr. Bernard Tribollet, from UPR 15 du CNRS (Paris) for critically reading the paper and for his useful suggestions.

References

R.S. Lillard, P.J. Moran and H.S. Isaacs, *J. Electrochem. Soc.* 139 (1992), p. 1007.

R.S. Lillard, J. Kruger, W.S. Tait and P.J. Moran, *Corrosion* 51 (1995), p. 251.

I. Annergren, D. Thierry and F. Zou, *J. Electrochem. Soc.* 144 (1997), p. 1208.

F. Zou and D. Thierry, *Electrochim. Acta* 42 (1997), p. 3293.

E. Bayet, F. Huet, M. Keddam, K. Ogle and H. Takenouti, *J. Electrochem. Soc.* 144 (1997), p. L87.

E. Bayet, F. Huet, M. Keddam, K. Ogle and H. Takenouti, *Electrochim. Acta* 44 (1999), p. 4117.

A.M. Mierisch, J. Yuan, R.G. Kelly and S.R. Taylor, *J. Electrochem. Soc.* 146 (1999), p. 4449.

L.V.S. Philippe, G.W. Walter and S.B. Lyon, *J. Electrochem. Soc.* 150 (2003), p. B111.

A.M. Mierisch and S.R. Taylor, *J. Electrochem. Soc.* 150 (2003), p. B303.

G. Baril, C. Blanc, M. Keddam and N. Pébère, *J. Electrochem. Soc.* 150 (2003), p. B488.

J.-B. Jorcin, E. Aragon, N. Pébère, in: Proceedings of the EUROCORR Symposium, CDRom, paper no. 02-418, 2004, pp. 1–10.

T. Missawa, K. Hashimoto and S. Shimodaira, *Corros. Sci.* 14 (1974), p. 131.

D. You, N. Pébère and F. Dabosi, *Corros. Sci.* 34 (1993), p. 5.

L. Bousselmi, C. Fiaud, B. Tribollet and E. Triki, *Corros. Sci.* 39 (1997), p. 1711.

L. Bousselmi, C. Fiaud, B. Tribollet and E. Triki, *Electrochim. Acta* 44 (1999), p. 4357.

I. Frateur, C. Deslouis, M.E. Orazem and B. Tribollet, *Electrochim. Acta* 44 (1999), p. 4345.

J.B. Jorcin, M.E. Orazem, N. Pébère, B. Tribollet, Electrochim. Acta, in press.

L. Beaunier, I. Epelboin, J.C. Lestrade and H. Takenouti, *Surf. Technol.* 4 (1976), p. 237.

B.A. Boukamp, *Solid State Ionics* 20 (1986), p. 31.

G.J. Brug, A.L.G. Van Den Eeden, M. Sluyters-Rehbach and J.H. Sluyters, *J. Electroanal. Chem.* 176 (1984), p. 275.

J.P. Quintela, R.C.A. De Oliveira, I.C.P. Margarit, O.R. Mattos, 192–194 (1995) 305.

D.H. van der Weijde, E.P.M. van Westing and J.H.W. de Wit, *Electrochim. Acta* 7/8 (1996), p. 1103.

W. Funke, *Prog. Org. Coat.* 9 (1981), p. 29.

J.H.W. de Wit In: P. Marcus and J. Oudar, Editors, *Corrosion Mechanisms in Theory and Practice*, Marcel Dekker Inc., New York (1995).

K. Barton, S. Bartonova and E. Beranek, *Werkst. Korros.* 25 (1974), p. 659.

M. Rohwerder, E. Hornung and M. Stratmann, *Electrochim. Acta* 48 (2003), p. 1235.

Corresponding author. Tel.: +33 5 6288 5665; fax: +33 5 6288 5663.

Original text : Elsevier.com